Physica C 471 (2011) 12–18

Contents lists available at ScienceDirect

Physica C

journal homepage: www.elsevier.com/locate/physc

Stability analysis for axially-symmetric magnetic field levitation of a superconducting sphere

S.N. Patitsas *

University of Lethbridge, 4401 University Drive, Lethbridge AB, Canada T1K3M4

ARTICLE INFO

Article history:
Received 14 September 2010
Received in revised form 10 October 2010
Accepted 13 October 2010
Available online 21 October 2010

Keywords:
Magnetic levitation
Superconducting sphere
Superconducting suspension
Stability analysis

ABSTRACT

For a magnetically levitated superconducting sphere, the stability analysis in both axial and radial directions is analyzed theoretically using a direct boundary-value problem approach. The external magnetic field is produced by a system of current-carrying coils with axial symmetry. We also assume complete exclusion of magnetic fields from the interior of the superconductor. Use of the P_l^1 associated Legendre functions as a basis set allows for a simple series solution for the magnetic stiffness coefficients as tridiagonal quadratic forms in terms of the expansion coefficients. Analysis shows that stability for this problem is not guaranteed in general. Stability is guaranteed though, if coil windings are designed in such away that all but one of the expansion coefficients are zero. Further cases with two and three non-zero coefficients are also solved. In particular the important 1, 3 and 2, 4 cases are treated in detail, and stability maps have been produced. Finally, the case where levitation is attempted by one pair of discrete current coils has been solved and stability mapping has been thoroughly explored.

1. Introduction

Earnshaw proved that stable levitation of a charge by a static external electric field is impossible, a direct result of the inverse square dependence of the electrostatic force [1,2]. Solutions to Laplace's equation allow saddle points but not local extrema in all directions. Subsequently, a similar result was established for magnetostatics though it was pointed out that stable levitation is possible if diamagnetic materials are present in the system [3]. As perfect diamagnets, superconductors are included within this class of materials. It is important to understand from these very general considerations that stable levitation may be possible, but by no means guaranteed for a given system.

Work towards stable magnetic levitation of objects has many possible applications including high speed, low friction bearings for gyroscopes, energy storage flywheels, centrifuges, etc. Also low noise suspension for sensitive scientific measurements, and energy efficient high speed train systems [3]. Stability analysis is essential for efficient design of magnetically levitated systems. Not only is avoiding instability crucially important, but even for stable systems, optimization of the stiffness in all directions is highly desired.

Stable magnetic levitation of a superconductor was first achieved in 1947 by Arkadiev [4]. Magnetic levitation of superconducting spheres has been demonstrated for the case of a solid lead sphere at 4.2 K levitated by a two-coil configuration [5] as well as solid niobium sphere, levitated in vacuum at 4.2 K, using a two-coil, and eight-coil unsymmetrical configuration [6].

Though analytical approaches have been reported using the method of images [7–9], small sphere limiting case [10] and the method of secondary sources [11,12], more recent studies have indicated that these approaches are unnecessarily complicated and have focused on taking a numerical calculation approach [13,14]. These treatments assume exclusion of all magnetic flux from the interior of the superconductor (Meissner effect) [15].

In this report the stability analysis in both axial and radial directions, of a levitated superconducting sphere is analyzed theoretically using a direct boundary-value problem approach based on the vector potential. The external magnetic field is produced by a system of current-carrying coils with axial symmetry. We also assume complete exclusion of magnetic fields from the interior of the superconductor. The problem is simplified significantly by a choice of the P_l^1 associated Legendre functions as a basis set with which to expand the current distribution. This leads to very simple expressions for the magnetic stiffness coefficients [3] in terms of the expansion coefficients.

It should be noted that the assumption of complete magnetic field exclusion can fail in some important scenarios. For example, it has been pointed out that when treating the forces on a superconducting magnet that is small enough to be used in a magnetic force microscope, then the London penetration depth must be accounted for [16]. Also, the assumption of complete expulsion of the magnetic field is correct for type-II superconductors only when

* Tel.: +1 403 329 2358.
E-mail address: steve.patitsas@uleth.ca

0921-4534/$ - see front matter © 2010 Elsevier B.V. All rights reserved.
doi:10.1016/j.physc.2010.10.003

the magnetic field is below the lower critical field B_{c1} [17]. Above B_{c1} the force calculations must be modified by including the energy of flux vortices [18]. As well, it is known that flux-pinning in type-II superconductors introduces hysteretic effects that can strongly effect the stability of levitated systems [18,19].

External forces such as gravity are not treated here. These results presented here are applicable either in a zero-gravity environment or in the case where the magnetic system is very stiff so that external forces that are present would have very small effects. Given a trend towards producing stronger and stronger fields [20,2] this is a reasonable approach for such systems.

2. Theory for stiffness coefficients

The net force on the superconducting sphere is calculated using the magnetic stress method [3]. Forces at the surface of the superconductor are always repulsive and surface normal [3]. In this discussion the term external force refers only to that caused by the coil current. Inclusion of any other very small external force would change the equilibrium position and stiffness constants by very small amounts. This is the case when the magnetic forces are very strong and stiff compared to everything else. When the magnetic field inside the superconducting sphere is zero, the net force on the sphere may be expressed in terms of an integral over the surface of the surface current density $\vec{K}_s$:

$$\vec{F}_s = -\frac{\mu_0}{2}\int K_s^2 \hat{r}_s\, da_s \tag{1}$$

where $\hat{r}_s$ is the radial unit vector [3]. Here we assume that the surface current density can be expressed in spherical polar components as $\vec{K}_s = K_\theta\hat{\theta} + K_\phi\hat{\phi}$ and is set up as a response to the applied fields produced by the coil. We consider the field source as a surface current density $\vec{K}_c$ on a larger sphere of radius b, as is illustrated in Fig. 1.

Here we report results for the restricted case where the current flows azimuthally around the z-axis. Otherwise this current is expressed as generally as possible with magnitude a function of the polar angle θ_c. In general the two spheres will be centered at two distinct points, differing by a vector $\vec{\eta}$. First we will calculate expressions for the fields when the spheres are concentric. From these expressions the net force can be calculated and conditions for equilibrium established. Then we will use a first order Taylor expansion of the magnetic field from the coil in order to find the net force to first order in $\vec{\eta}$. This directly gives the stiffness constants in the axial and lateral directions.

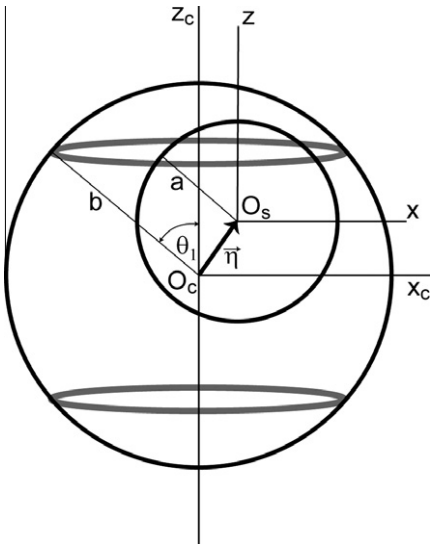

Fig. 1. Schematic diagram of the superconducting sphere inner with radius a, translated from the coil origin by vector η. Two grey coils are indicated on the coil sphere at polar angle θ_1.

To zeroth order in $\vec{\eta}$, $\vec{K}_s$ is purely azimuthal, i.e. $K_\theta = 0$. The net force is:

$$\vec{F}_0 \cdot \hat{\eta} = -\frac{\mu_0}{2}\int \left(K_\phi|_0\right)^2 (\hat{r}_s \cdot \hat{\eta})\, da_s \tag{2}$$

and the stiffness coefficients in the z- and x-directions are:

$$k_z = \mu_0 \int K_\phi|_0 \left.\frac{\partial K_\phi}{\partial z}\right|_0 (\hat{r}_s \cdot \hat{z})\, da_s \tag{3}$$

$$k_x = \mu_0 \int K_\phi|_0 \left.\frac{\partial K_\phi}{\partial x}\right|_0 (\hat{r}_s \cdot \hat{x})\, da_s \tag{4}$$

2.1. The external field

The function K_c can be expanded as a linear superposition of associated Legendre functions P_l^1 as:

$$K_c(\theta_c) = \sum_{l=1}^{\infty} c_l P_l^1(\cos\theta_c) \tag{5}$$

The reason for this particular set of complete functions will be made clear in this section. The magnetic vector potential function at the field point $\vec{r}$ can be expressed as a spherical surface integral over source points $\vec{r}_c$ at radius b:

$$\vec{A}_c = \frac{\mu_0}{4\pi}\int \frac{\vec{K}_c}{|\vec{r}-\vec{r}_c|}\, da_c \tag{6}$$

with $\vec{K}_c = K_c(\theta_c)\hat{\phi}_c = K_c(\theta_c)[-\sin\phi_c\hat{x} + \cos\phi_c\hat{y}]$. For $r_c = b > r$ one can use the multipole expansion formula:

$$\frac{1}{|\vec{r}-\vec{r}_c|} = \sum_{l=0}^{\infty} \frac{r^l}{b^{l+1}} P_l(\cos\gamma) \tag{7}$$

as well as the addition formula [21,22]:

$$P_l(\cos\gamma) = P_l(\cos\theta)P_l(\cos\theta_c) + 2\sum_{m=1}^{l} \times \frac{(l-m)!}{(l+m)!} P_l^m(\cos\theta)P_l^m(\cos\theta_c)\cos[m(\phi-\phi_c)] \tag{8}$$

Making use of the azimuthal unit vector:

$$\hat{\phi}_c = -\sin\phi_c\hat{x} + \cos\phi_c\hat{y} \tag{9}$$

we see that only the $m = 1$ term is contributing. Using the orthogonality of the P_l^1 functions:

$$\int_0^{\pi} \sin\theta P_l^1(\cos\theta)P_n^1(\cos\theta)d\theta = \frac{2l(l+1)}{2l+1}\delta_{ln} \tag{10}$$

results in the following expression for $\vec{A}_c$, valid for $r < b$:

$$\vec{A}_c = \mu_0 \sum_{l=1}^{\infty} c_l \frac{1}{2l+1}\frac{r^l}{b^{l-1}} P_l^1(\cos\theta)\hat{\phi} \tag{11}$$

The $m = 1$ associated Legendre functions arise naturally in this class of magnetostatic problems, as in the classic example of a single circular current loop [21,22]. This makes the P_l^1 functions a good choice for our basis set. By direct application of the curl vector derivative and use of standard recurrence relations for the associated Legendre polynomials the magnetic field is calculated. One such useful recurrence relation is [22]:

$$\frac{\partial}{\partial\theta}\left(\sin\theta P_l^1(\cos\theta)\right) = -l(l+1)\sin\theta P_l^0(\cos\theta) \tag{12}$$

The result for the magnetic field produced by the coil is:

$$\vec{B}_c = -\mu_0 \sum_{l=1}^{\infty} c_l \frac{l+1}{2l+1} \frac{r^{l-1}}{b^{l-1}} \left[l P_l^0(\cos\theta)\hat{r} + P_l^1(\cos\theta)\hat{\theta} \right] \tag{13}$$

2.2. Shifting the fields

Direct differentiation followed with further use of the following recurrence relation:

$$\sin\theta \frac{d}{d\theta} P_l^1(\cos\theta) = l\cos\theta P_l^1(\cos\theta) - (l+1) P_{l-1}^1(\cos\theta) \tag{14}$$

gives:

$$\frac{\partial \vec{B}_c}{\partial z} = -\mu_0 \sum_{l=2}^{\infty} c_l \frac{l(l+1)}{2l+1} \times \frac{r^{l-2}}{b^{l-1}} \left[(l-1) P_{l-1}^0(\cos\theta)\hat{r} + P_{l-1}^1(\cos\theta)\hat{\theta} \right] \tag{15}$$

$$\frac{\partial \vec{B}_c}{\partial x} = -\mu_0 \sum_{l=2}^{\infty} c_l \frac{(l+1)}{2l+1} \frac{r^{l-2}}{b^{l-1}} \left[(l-1) P_{l-1}^1(\cos\theta)\cos\phi\hat{r} + \left(\frac{d}{d\theta} P_{l-1}^1(\cos\theta) \right) \cos\phi\hat{\theta} - \frac{P_{l-1}^1(\cos\theta)}{\sin\theta} \sin\phi\hat{\phi} \right] \tag{16}$$

In all terms the index l has been reduced by one. The surface currents $\vec{K}_s$ create a magnetic field $\vec{B}$ such that the net field $\vec{B} + \vec{B}_c$ is zero for $r < a$. With no loss of generality we take the displacement vector $\vec{\eta}$ to lie in the xz plane. To first order in $\vec{\eta}$ the response field is given by:

$$\begin{aligned} \vec{B} = {} & \mu_0 \sum_{l=1}^{\infty} \frac{(l+1)c_l}{(2l+1)b^{l-1}} r^{l-1} \left[l P_l^0(\cos\theta)\hat{r} + P_l^1(\cos\theta)\hat{\theta} \right] \\ & + \mu_0 \sum_{l=2}^{\infty} \frac{(l+1)c_l}{(2l+1)b^{l-1}} \left\{ \eta_z \, l r^{l-2} \left[(l-1) P_{l-1}^0(\cos\theta)\hat{r} + P_{l-1}^1(\cos\theta)\hat{\theta} \right] \right. \\ & + \eta_x r^{l-2} \left[(l-1) P_{l-1}^1(\cos\theta)\cos\phi\hat{r} + \left(\frac{d}{d\theta} P_{l-1}^1(\cos\theta) \right) \cos\phi\hat{\theta} \right. \\ & \left. \left. - \frac{1}{\sin\theta} P_{l-1}^1(\cos\theta)\sin\phi\hat{\phi} \right] \right\} \end{aligned} \tag{17}$$

for $r < a$, while ensuring a zero-curl field just outside the inner sphere gives:

$$\begin{aligned} \vec{B} = {} & \mu_0 \sum_{l=1}^{\infty} \frac{(l+1)c_l}{(2l+1)b^{l-1}} \frac{a^{2l+1}}{r^{l+2}} l \left[P_l^0(\cos\theta)\hat{r} - \frac{1}{l+1} P_l^1(\cos\theta)\hat{\theta} \right] \\ & + \sum_{l=1}^{\infty} \frac{(l+1)c_l a^{2l-1}}{(2l+1)b^{l-1} r^{l+1}} \left\{ \eta_z (l-1) \left[l P_{l-1}^0(\cos\theta)\hat{r} - P_{l-1}^1(\cos\theta)\hat{\theta} \right] \right. \\ & + \eta_x \frac{(l-1)}{l} \left[l P_{l-1}^1(\cos\theta)\cos\phi\hat{r} - \left(\frac{d}{d\theta} P_{l-1}^1(\cos\theta) \right) \cos\phi\hat{\theta} \right. \\ & \left. \left. + \frac{1}{\sin\theta} P_{l-1}^1(\cos\theta)\sin\phi\hat{\phi} \right] \right\} \end{aligned} \tag{18}$$

for $r > a$. The normal component of $\vec{B}$ is continuous at $r = a$ while the lateral components have discontinuities related to the surface currents. In particular $K_\phi = (B_{out} - B_{in})_\theta / \mu_0$. The discontinuities follow the standard $2l+1$ rule [22,23]. Thus

$$K_\phi|_0 = -\sum_{l=1}^{\infty} c_l \left(\frac{a}{b} \right)^{l-1} P_l^1(\cos\theta) \tag{19}$$

$$\left. \frac{dK_\phi}{d\eta_z} \right|_0 = -\sum_{l=2}^{\infty} c_l \left(\frac{a^{l-2}}{b^{l-1}} \right) (l+1) \frac{2l-1}{2l+1} P_{l-1}^1(\cos\theta) \tag{20}$$

$$\left. \frac{dK_\phi}{d\eta_x} \right|_0 = -\sum_{l=2}^{\infty} c_l \left(\frac{a^{l-2}}{b^{l-1}} \right) \frac{(l+1)}{l} \frac{2l-1}{2l+1} \left(\frac{d}{d\theta} P_{l-1}^1(\cos\theta) \right) \cos\phi \tag{21}$$

To evaluate k_z using Eq. (3) with $\hat{r}\cdot\hat{z} = \cos\theta$ we make use of the following recurrence relation:

$$\cos\theta P_{l-1}^1(\cos\theta) = \frac{l-1}{2l-1} P_l^1(\cos\theta) + \frac{l}{2l-1} P_{l-2}^1(\cos\theta) \tag{22}$$

Subsequent use of Eq. (10) gives the desired result:

$$k_z = 4\pi\mu_0 a \sum_{l=2}^{\infty} \frac{(l-1)l(l+1)}{(2l+1)} \left(\frac{a}{b} \right)^{2l-4} \left[\frac{l+1}{2l+1} \frac{a^2}{b^2} c_l^2 + \frac{(l-2)}{(2l-3)} c_l c_{l-2} \right] \tag{23}$$

To evaluate k_x using (4) with $\hat{r}\cdot\hat{x} = \sin\theta\cos\phi$ we make use of the following recurrence relation:

$$\sin\theta \frac{d}{d\theta} P_{l-1}^1(\cos\theta) = \frac{(l-1)^2}{2l-1} P_l^1(\cos\theta) - \frac{l^2}{2l-1} P_{l-2}^1(\cos\theta) \tag{24}$$

to give:

$$k_x = 2\pi\mu_0 a \sum_{l=2}^{\infty} \frac{(l-1)(l+1)}{(2l+1)} \left(\frac{a}{b} \right)^{2l-4} \left[\frac{(l+1)(l-1)}{2l+1} \frac{a^2}{b^2} c_l^2 - \frac{(l-2)l}{(2l-3)} c_l c_{l-2} \right] \tag{25}$$

Incidentally, the force to zeroth order is given by

$$\vec{F}\Big|_0 = -2\pi\mu_0 a^2 \sum_{l=1}^{\infty} \frac{l(l+1)}{(2l+1)} \left(\frac{a}{b} \right)^{2l-1} c_l c_{l+1} \hat{z} \tag{26}$$

For convenience we define

$$d_l \equiv \frac{l(l+1)}{2l+1} \left(\frac{a}{b} \right)^l c_l \tag{27}$$

which allows for a more concise expression of the stiffness:

$$\frac{k_z a}{4\pi\mu_0 b^2} = \sum_{l=2}^{\infty} \left[\left(\frac{l-1}{l} \right) d_l^2 + d_l d_{l-2} \right] \tag{28}$$

$$\frac{k_x a}{4\pi\mu_0 b^2} = \frac{1}{2} \sum_{l=2}^{\infty} \left[\left(\frac{l-1}{l} \right)^2 d_l^2 - d_l d_{l-2} \right] \tag{29}$$

Inspection of Eq. (26) shows that setting $c_l c_{l-1} = 0$ for all l is a sufficient condition for equilibrium at $\vec{\eta} = 0$. This leads one to adopt either an all odd-l or all even-l coil current configuration, as will be the case from here on. For this reason the use here on of the term *consecutive* means that the two integers differ by two ex. 3,5.

3. Results for odd and even series

For the case where only odd-l terms are non-zero, Eqs. (28) and (29) are quadratic forms in terms of the vector $|\mathbf{d}\rangle$, i.e.

$$\frac{k_z a}{4\pi\mu_0 b^2} = \langle \mathbf{d} | \mathbf{Z_{odd}} | \mathbf{d} \rangle \tag{30}$$

$$\frac{k_x a}{4\pi\mu_0 b^2} = \frac{1}{2} \langle \mathbf{d} | \mathbf{X_{odd}} | \mathbf{d} \rangle \tag{31}$$

where the representations for $\mathbf{Z_{odd}}$ and $\mathbf{X_{odd}}$ are real symmetric tridiagonal matrices:

$$\mathbf{Z_{odd}} = \begin{pmatrix} 0 & \frac{1}{2} & 0 & 0 & \cdots \\ \frac{1}{2} & \frac{2}{3} & \frac{1}{2} & 0 & \cdots \\ 0 & \frac{1}{2} & \frac{4}{5} & \frac{1}{2} & \cdots \\ 0 & 0 & \frac{1}{2} & \frac{6}{7} & \cdots \\ \vdots & \vdots & \vdots & \vdots & \end{pmatrix} \tag{32}$$

$$\mathbf{X_{odd}} = \begin{pmatrix} 0 & -\frac{1}{2} & 0 & 0 & \cdots \\ -\frac{1}{2} & \frac{2^2}{3^2} & -\frac{1}{2} & 0 & \cdots \\ 0 & -\frac{1}{2} & \frac{4^2}{5^2} & -\frac{1}{2} & \cdots \\ 0 & 0 & -\frac{1}{2} & \frac{6^2}{7^2} & \cdots \\ \vdots & \vdots & \vdots & \vdots & \end{pmatrix} \tag{33}$$

Mechanical stability is then determined by the signs of the eigenvalues of these matrices. The existence of even one negative eigenvalue in either matrix means that a set of coefficients c_l can be found that will lead to instability. We have used numerical calculations to show that both of these matrices do indeed possess such negative eigenvalues. Truncating $\mathbf{X_{odd}}$ even at $N = 5$ gives a set of eigenvalues with 1 that is negative with a value of ~ -0.43557. Truncating $\mathbf{X_{odd}}$ at $N = 20$ gives a set of eigenvalues with 3 that are negative and an overall set minimum value of ~ -0.437483. Truncating $\mathbf{X_{odd}}$ at $N = 100$ gives a set of eigenvalues with 7 that are negative and a converged minimum value of ~ -0.437483. For the case $N = 20$ the eigenvector (actually c_l) corresponding to the lowest eigenvalue is shown in Fig. 2 for three values of the ratio b/a. In this case a threshold value for this ratio of about 2.465 is obtained. Smaller (larger) b/a values give a solution with c_l that falls off (rises) approximately exponentially with l. The usefulness of this stability analysis is demonstrated here: If any of the three configurations shown in Fig. 2 were to be created from a given experimental construction of a current coil, it would be difficult to realize *a priori* that instability would result.

For the case of the even-l only series the matrices are given by:

$$\mathbf{Z_{even}} = \begin{pmatrix} \frac{1}{2} & \frac{1}{2} & 0 & 0 & \cdots \\ \frac{1}{2} & \frac{3}{4} & \frac{1}{2} & 0 & \cdots \\ 0 & \frac{1}{2} & \frac{5}{6} & \frac{1}{2} & \cdots \\ 0 & 0 & \frac{1}{2} & \frac{7}{8} & \cdots \\ \vdots & \vdots & \vdots & \vdots & \end{pmatrix} \tag{34}$$

and

$$\mathbf{X_{even}} = \begin{pmatrix} \frac{1}{4} & -\frac{1}{2} & 0 & 0 & \cdots \\ -\frac{1}{2} & \frac{3^2}{4^2} & -\frac{1}{2} & 0 & \cdots \\ 0 & -\frac{1}{2} & \frac{5^2}{6^2} & -\frac{1}{2} & \cdots \\ 0 & 0 & -\frac{1}{2} & \frac{7^2}{8^2} & \cdots \\ \vdots & \vdots & \vdots & \vdots & \end{pmatrix} \tag{35}$$

These matrices also have negative eigenvalues, as verified by numerical computation, thus making the even-l only scenario inherently unstable as well.

4. Single non-zero coefficient

Here the special case is considered where just one c_l value is non-zero. In this case off-diagonal matrix elements are irrelevant. For $l > 1$, clearly both k_z and k_x are positive definite, thus ensuring stability. The special case of $l = 1$ gives the well-known result [23] of the coil producing a uniform magnetic field inside the coil, hence neutral equilibrium. For $l = 2$ $k_z = 4\pi\mu_0(18a^3/25b^2)c_2^2$ and $k_x = k_z/4$. For large l, $k_z \approx \pi\mu_0 a\, l^2(a/b)^{2l-2}$ while $k_x = 2l\, k_z/(l-1) \approx k_z/2$.

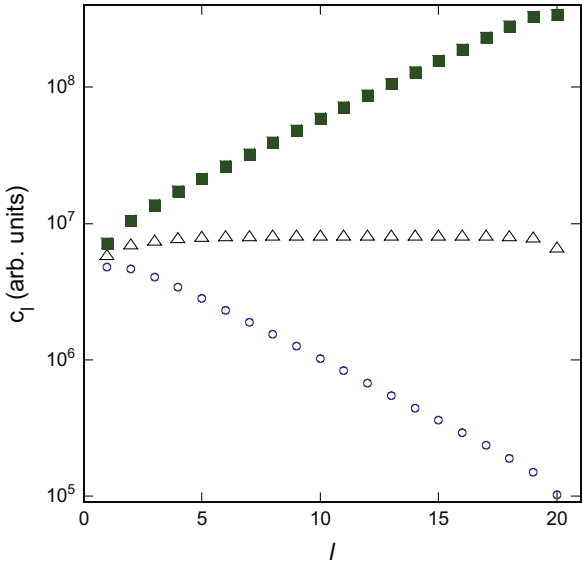

Fig. 2. Eigenvector set of coefficients c_l vs. l for the most negative eigenvector of the matrix $\mathbf{X_{odd}}$, truncated to $N = 20$. Eigenvectors are not normalized. From the one set d_l, three representative sets c_l are calculated for $b/a = 2$ (open blue circles), $b/a = 2.465$ (open black triangles), $b/a = 3$ (filled green squares). (For interpretation of the references to color in this figure legend, the reader is referred to the web version of this article.)

As yet, reported levitation designs have a small number of coils, the most that we are aware of is eight [6]. The two-coil system will be discussed in Section 7. Future designs, however, with more powerful magnetic fields [20,2] and stiffness coefficients in mind, will likely have many coils. With options for varying the density of coils as well as the current carried by each, one can in principle design a system to produce just one non-zero c_l coefficient. This is an ideal situation; in practice other non-zero coefficients may also exist. If the coefficients are not consecutive then the effect is simply additive. Though many possibilities exist, we will next discuss two simple cases involving consecutive coefficients.

5. Two consecutive non-zero coefficients

When the only non-zero coefficients are the two consecutive terms, d_{l-2} and d_l, then by simple completion of squares we see that:

$$\frac{k_z a}{4\pi\mu_0 b^2} = \frac{l-1}{l}\left[d_l + \frac{l d_{l-2}}{2l-2}\right]^2 + \frac{3}{4}\frac{d_{l-2}^2}{(l-1)(l-2)} g_z(l) \tag{36}$$

with

$$g_z(l) = \left(l - \frac{7}{3}\right)^2 - \frac{13}{9} \tag{37}$$

The function g_z is positive for $l \geqslant 4$ so stability in the z-direction is guaranteed for $l \geqslant 4$. For the off-axial motion:

$$\frac{k_x a}{2\pi\mu_0 b^2} = \left[\frac{l-1}{l} d_l - \frac{l}{2l-2} d_{l-2}\right]^2 + \frac{3}{4}\left(\frac{d_{l-2}^2}{(l-1)(l-2)}\right)^2 g_x(l) \tag{38}$$

with

$$g_x(l) = \left(l^2 - 6l + 6\right)\left(l^2 - \frac{10}{3}l + 2\right) \tag{39}$$

For $l \geqslant 5$, g_x is a positive function while $g_x(3) = -3$ and $g_x(4) = -28/3$. For the case of two consecutive terms, overall stability is guaranteed if $l \geqslant 5$, i.e. for the cases 3, 5 and up, stability is guaranteed.

Explicitly for the 1, 3 case:

$$k_z = \frac{32\pi\mu_0}{49}\frac{a^4}{b^3}c_3\left[12\frac{a}{b}c_3 + 7\frac{b}{a}c_1\right] \tag{40}$$

$$k_x = \frac{16\pi\mu_0}{49}\frac{a^4}{b^3}c_3\left[8\frac{a}{b}c_3 - 7\frac{b}{a}c_1\right] \tag{41}$$

From Eq. (40) the condition $k_z = 0$ implies that the ratio, r, of $\frac{a}{b}c_3$ to $\frac{b}{a}c_1$ will take on the two possible values: 0 and $-7/12$. These two slope values demarcate the region of lateral instability in the plot shown in Fig. 3. Also shown are the two slope values $r = 0$ and $r = 7/8$ at which $k_x = 0$, as well as the two slope values $r = 0$ and $r = -21/16$ at which $k_x = k_z$ (dashed line).

For the 2, 4 case explicitly:

$$k_z = \frac{16\pi\mu_0}{3}\frac{a^5}{b^4}\left\{\left[\frac{5a}{3b}c_4 + \frac{3b}{5a}c_2\right]^2 + \frac{9}{2}\left(\frac{bc_2}{5a}\right)^2\right\} \tag{42}$$

$$k_x = 2\pi\mu_0\frac{a^5}{b^4}\left\{\left[\frac{5a}{3b}c_4 - \frac{4b}{5a}c_2\right]^2 - 7\left(\frac{bc_2}{5a}\right)^2\right\} \tag{43}$$

From Eq. (43) the condition $k_x = 0$ implies that the ratio, r, of $\frac{a}{b}c_4$ to $\frac{b}{a}c_2$ will take on the two possible values: $\frac{3}{25}(4 \pm \sqrt{7})$. These two slope values demarcate the region of instability in the plot shown in Fig. 4. Also, inspection of Eq. (42) shows that motion in the axial direction is softest when $r = -\frac{9}{25}$ (dashed line).

6. Three consecutive non-zero coefficients

Qualitatively, the results are similar to the case of two consecutive terms: when the l-value is large enough stability is guaranteed, as determined from numerical computation. The only cases with instabilities are now listed: For the 1, 3, 5 case and the 2, 4, 6 case both k_z and k_x can be negative. For the 3, 5, 7 case and for the 4, 6, 8 case k_x can be negative.

7. Single pair of loops

In this section we consider what happens when the coil surface current K_c is concentrated down to a series of discrete loops, similar to the experimental conditions discussed in Refs. [5,6]. In particular consider two such discrete coils, with one coil carrying current I_1 flowing counter-clockwise at polar angle $+\theta_1$ and another at $\pi - \theta_1$ with polarity $(-1)^p$, $(p = 0,1)$, so that the surface current is expressed as:

$$K_c(\theta) = \frac{I_1}{b}\delta(\theta - \theta_1) + (-1)^p\frac{I_1}{b}\delta(\theta + \theta_1 - \pi) \tag{44}$$

Using Eqs. (5) and (10) the coefficients c_l are

$$c_l = \frac{f_{pl}I_1\sin\theta_1}{b}\frac{2l+1}{l(l+1)}P_l^1(\cos\theta_1) \tag{45}$$

where $f_{pl} = [1 - (-1)^{p+l+1}]/2$ takes values 0 or 1. For $p = 1$ ($p = 0$) only odd (even) l terms will contribute. Either p value ensures zero net force.

As an example consider the case $p = 1$ and $a \ll b$. In this case the leading term for the spring constants (Eqs. (23) and (25)) is the 1, 3 cross-term, i.e.

$$k_z = 6\pi\mu_0\frac{a^3}{b^4}I_1^2\sin^4\theta_1(5\cos^2\theta_1 - 1) \tag{46}$$

and $k_x = -k_z/2$, which makes stable equilibrium impossible. Note also that both stiffness constants are zero at the condition $\theta_1 = \tan^{-1}(2)$, or $\theta_1 = 63.4°$, the same as for the well-known Helmholtz coil. For the purposes of achieving stable and stiff levitation, odd l configurations are unfavourable, at least for small superconducting spheres.

For $p = 0$, i.e. even l and $a \ll b$ the leading term is $l = 2$:

$$k_z = 18\pi\mu_0\frac{a^3}{b^4}I_1^2\sin^4\theta_1\cos^2\theta_1 \tag{47}$$

and $k_x = +k_z/4$. Stability is ensured for the full range $0 < \theta_1 < \pi/2$. The field produced at the origin is zero, so stable levitation of a small superconducting sphere makes sense; the diamagnetic sphere is repelled from the stronger fields existing away from the origin.

These examples are instructive but levitation configurations involving heavy loads or maximal stiffness are likely to have the inner radius a slightly smaller than radius b so many terms need to be included. As a small step in this direction consider the 2, 4 only case with $c_2 = 5I_1\sin\theta_1 P_2^1(\cos\theta_1)/(6b)$ and $c_4 = 9I_1\sin\theta_1 P_4^1(\cos\theta_1)/(20b)$. Inspection of (43) and Fig. 4 shows that instability is possible, depending on the choice of θ_1.

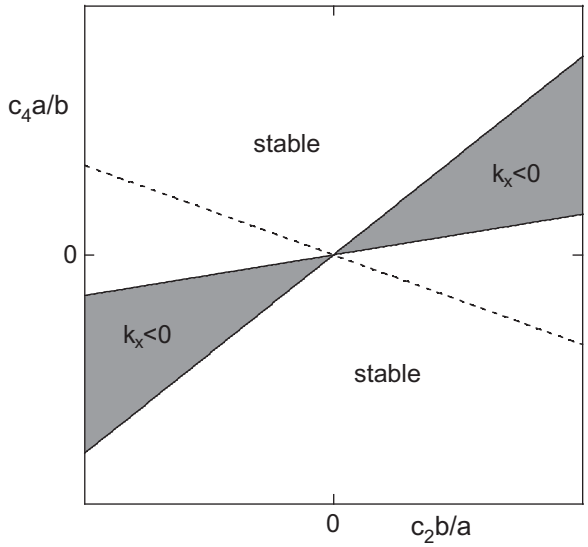

Fig. 4. Stability diagram for the case where only c_2 and c_4 are non-zero. Regions of lateral instability are shaded and the dashed line shows where k_z is soft.

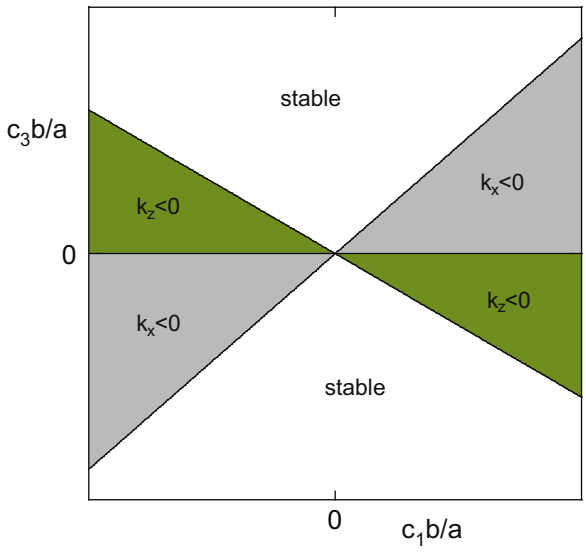

Fig. 3. Stability diagram for the case where only c_1 and c_3 are non-zero. Regions of instability are shaded (light grey for lateral instability, dark green for axial instability). (For interpretation of the references to color in this figure legend, the reader is referred to the web version of this article.)

7.1. Numerical results for one pair of loops

To proceed further, numerical computations of k_z and k_x are easily accomplished after combining Eqs. (23), (25) and (45). One example is shown in Fig. 5 for the even-l case with $a = 0.7b$. Here the functions $4\pi k_z b/(\mu_0 I_1^2)$ and $4\pi k_x b/(\mu_0 I_1^2)$ are plotted. Both k_z and k_x take negative values over some range. A region of stability exists from $\theta_1 = 38°$ to $\theta_1 = 69°$. The unstable regions make intuitive sense: For $\theta_1 < 38°$ where $k_x < 0$ the coils are located near the poles and the superconductor can escape by moving radially. For $\theta_1 > 69°$ where $k_z < 0$ the coils are located near the equator and the superconductor can escape by moving axially.

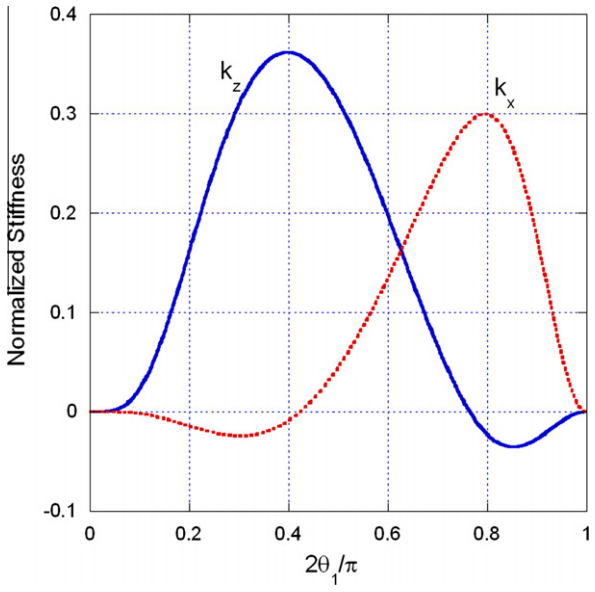

Fig. 5. Plots of stiffness parameters k_z (solid, blue) and k_x (dashed, red) vs. θ_1 for the case of a single coil pair ($p = 0$) with $a = 0.7b$. Both parameters are normalized by $\mu_0 I_1^2/(4\pi b)$. (For interpretation of the references to color in this figure legend, the reader is referred to the web version of this article.)

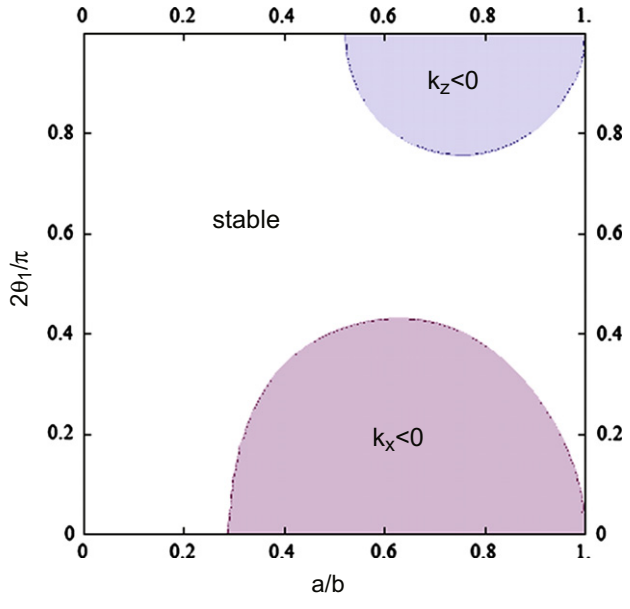

Fig. 6. Stability plot for the case of a single coil pair. The current distribution is antisymmetric so only even-l terms are present. The two free parameters left are a/b and θ_1.

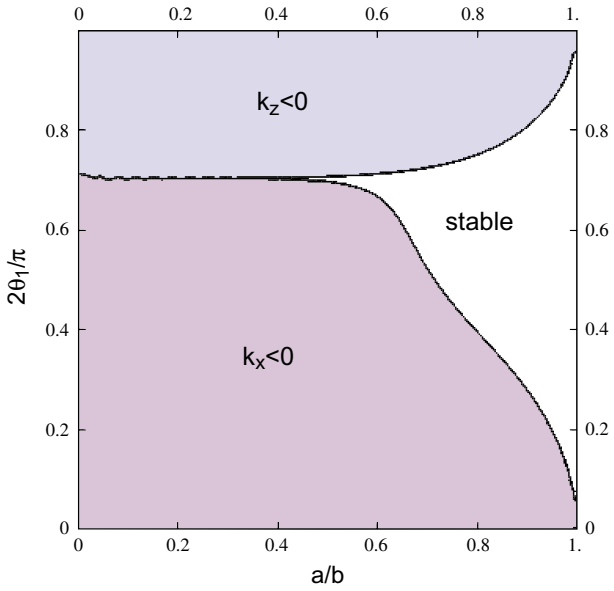

Fig. 7. Stability plot for the case of a single coil pair. The current distribution is symmetric (current in both loops in the same direction) so only odd-l terms are present.

The data presented in Fig. 5 can be projected down as a vertical slice of the stability plot presented in Fig. 6. In this plot θ_1 is plotted on the ordinate while a/b is varied on the abscissa. Two regions of instability are clearly delineated, one where $k_x < 0$, the other where $k_z < 0$. Overall, stability is easier to attain when a/b is small. In fact, for $a/b < 0.28$ we see that stability is ensured. However, in a practical levitation attempt to create high stiffness and/or strong lifting forces, one would like to choose a/b to not be so small. This plot can serve as a warning against using any calculation that assumes the levitating object is small (if indeed it is not) or against the temptation to view the square of the magnetic field as a potential energy function.

Finally, the stability plot for odd-l series (current in both loops in same direction) is shown in Fig. 7. One is at first struck by how the regions of axial and lateral instability fill most of the plot. Also verified is complete lack of opportunity for stable levitation for a small superconducting sphere ($a/b \lesssim 0.42$) with the $k_x = k_z = 0$ boundary located at the Helmholtz angle, $\theta_1 = 63.4°$. For larger values of a/b we see that the window of stable levitation opens up nicely. In fact when a approaches b designing a system with odd terms only is actually a workable option.

8. Conclusions

A vector potential based theoretical approach has been developed for calculating the magnetic force and stiffness coefficients for a superconducting sphere surrounded by an axially-symmetric electric current confined to the surface of a larger sphere. With a judicious choice of basis functions for expansion, simple analytic results are derived for the stiffness coefficients, and hence the stability. The stiffness has been expressed as tridiagonal quadratic forms in terms of the expansion coefficients. Stability for this problem is not guaranteed in general. In terms of the coil current expansion coefficients c_l we have found that if all are zero but one, then stability is guaranteed. For the case where all are zero save for two successive terms, we have outlined in detail the cases for stable or unstable levitation. In particular the 1, 3 and 2, 4 cases deserved special attention and the stability regions were mapped out. Lastly, the case of one pair of current coils was addressed as an example and non-trivial stability plots were presented. The

results presented here should be very useful when applied towards any future design of current winding configurations to be implemented in practical magnetic levitation. We anticipate using this approach in the future to aid in the design of magnetic levitation systems designed for filtering out mechanical noise.

Acknowledgements

We thank the Natural Sciences and Engineering Research Council of Canada for financial support of this work. We also thank Cathy J. Meyer for her determined efforts in editing this manuscript.

References

[1] S. Earnshaw, Transactions of the Cambridge Philosophical Society 7 (1842) 97–112.
[2] M. Simon, A.K. Geim, Diamagnetic levitation: flying frogs and floating magnets, Journal of Applied Physics 87 (2000) 6200.
[3] F.C. Moon, P.-Z. Chang, Superconducting Levitation, John Wiley & Sons, Inc., 1994.
[4] V. Arkadiev, A floating magnet, Nature 160 (1947) 330.
[5] I. Simon, Forces acting on superconductors in magnetic fields, Journal of Applied Physics 24 (1953) 1.
[6] J.T. Harding, R. Tuffias, The Cryogenic Gyro, Technical Release 34-100, NASA Jet Propulsion Laboratory, Pasadena, California, 1960.
[7] M. Levin, The solution of a problem in quasistationary electrodynamics by the method of images, Soviet Physics: Technical Physics 9 (1964) 312.
[8] A. Sezginer, Explanation of the superconducting suspension effect, Physical Review B 39 (1989) 9598.
[9] Q.-G. Lin, Physical Review B 74 (2006) 024510.
[10] V. Beloozorov, Confinement of a superconducting sphere by a system of ring currents, Soviet Physics: Technical Physics 11 (1966) 631.
[11] Y.M. Urman, Theory for the calculation of the force characteristics of an electromagnetic suspension of a superconducting body, Technical Physics 42 (1997) 1–6.
[12] Y.M. Urman, Calculation of the force characteristics of a multi-coil suspension of a superconducting sphere, Technical Physics 42 (1997) 7–13.
[13] C. He, Q. Wang, Force characteristics analysis on a superconducting sphere suspended by spherical coils, Cryogenics 47 (2007) 413.
[14] J. Liu, Q. Wang, L. Yan, Analysis of force characteristics of a superconducting ball in a given magnetic field, Physica C 469 (2009) 756.
[15] N.W. Ashcroft, D.N. Mermin, Solid State Physics, first ed., Thomson Learning, Toronto, 1996. ISBN:0030839939. <http://www.worldcat.org/isbn/0030839939>.
[16] J.H. Xu, J.H. Miller Jr., C.S. Ting, Magnetic levitation force and penetration depth in type-II superconductors, Physical Review B 51 (1995) 424.
[17] Z. Yang, T. Johansen, H. Bratsberg, A. Bhatnagar, A. Skjeltorp, Lifting forces on a cylindrical magnet above a superconducting plane, Physica C 197 (1992) 136–146.
[18] F. Hellman, E. Gyorgy, D. J Jr., H. O'Bryan, R. Sherwood, Levitation of a magnet over a flat type II superconductor, Journal of Applied Physics 63 (1988) 447.
[19] F. Moon, M. Yanoviak, R. Ware, Hysteretic levitation forces in superconducting ceramics, Applied Physics Letters 52 (1988) 1534.
[20] A.K. Geim, M. Simon, M. Boamfa, L. Heflinger, Nature 400 (1999) 323.
[21] G. Arfken, Mathematical Methods For Physicists, third ed., Academic Press, 1985.
[22] J.D. Jackson, Classical Electrodynamics, third ed., John Wiley & Sons, 1999.
[23] D.J. Griffiths, Introduction to Electrodynamics, third ed., Prentice Hall, 1999.